Laterally Electrostatically Driven Poly 3C-SiC Folded-Beam Resonant Microstructures*

Wang Liang[1,2,†], Zhao Yongmei[1,2], Ning Jin[2], Sun Guosheng[1,2], Wang Lei[1], Liu Xingfang[1,2], Zhao Wanshun[1], Zeng Yiping[1], and Li Jinmin[1]

(1 *Novel Semiconductor Material Laboratory, Institute of Semiconductors, Chinese Academy of Sciences, Beijing* 100083, *China*)
(2 *State Key Laboratory of Transducer Technology, Chinese Academy of Sciences, Beijing* 100083, *China*)

Abstract: Micromachined comb-drive electrostatic resonators with folded-cantilever beams were designed and fabricated. A combination of Rayleigh's method and finite-element analysis was used to calculate the resonant frequency drift as we adjusted the device geometry and material parameters. Three micromachined lateral resonant resonators with different beam widths were fabricated. Their resonant frequencies were experimentally measured to be 64.5, 147.2, and 255.5kHz, respectively, which are in good agreement with the simulated resonant frequency. It is shown that an improved frequency performance could be obtained on the poly 3C-SiC based device structural material systems with high Young's modulus.

Key words: lateral resonant device; folded-beam; comb structure; MEMS; resonator; silicon carbide
EEACC: 2575
CLC number: TN303 **Document code**: A **Article ID**: 0253-4177(2008)08-1453-04

1 Introduction

Micromachined resonators are emerging as potential on-chip replacements for conventional discrete oscillators and filters in high performance communication transceivers. Electrostatic excitation combined with capacitive (electrostatic) detection is an attractive approach for silicon microstructures because of its simplicity and compatibility with micromachining technology[1]. SiC is a wide band gap semiconductor material well known for its mechanical characteristics, such as high Young's modulus and chemical inertness, yield strength, high thermal conductivity, and electrical stability at temperatures well above 600℃[2]. The first two properties in particular make it an excellent material to fabricate high frequency and high quality factor MEMS devices. Several groups have reported the fabrication methods of MEMS and NEMS resonators. They used polysilicon[3], poly-SiC[4], and monocrystalline 3C-SiC[5] as the structure materials.

In this paper, we describe the design, fabrication, and initial testing of an electrostatic comb structure for exciting and sensing the vibration of poly 3C-SiC microstructures parallel to the plane of the substrate. A combination of Rayleigh's method and finite-element analysis is used to calculate the device resonant frequency as we adjust the device geometry and material parameters.

2 Theory and design

2.1 Electrostatic comb drive

Figure 1 shows the layout of a linear resonant structure that can be driven electrostatically from one side and sensed capacitively at the other side with interdigitated finger (comb) structures. If a capacitor is charged so that a voltage difference of V appears between its electrodes, the exerted electrostatic force on the electrodes, F_V, is found from:

$$F_V = \nabla W = \frac{V^2}{2} \nabla C \tag{1}$$

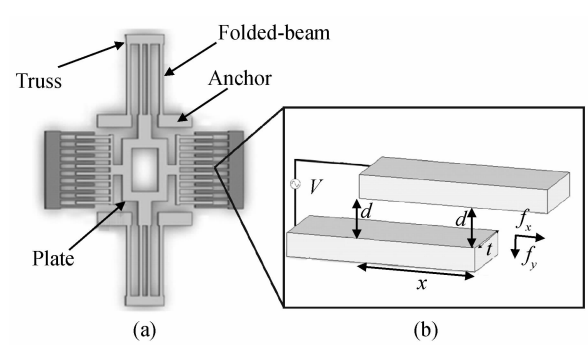

Fig. 1 (a) Layout of the linear resonant structure; (b) Enlarged view of the linear comb structure

* Project supported by the National Natural Science Foundation of China (No. 60406010) and the National High Technology Research and Development Program of China (No. 2006AA04Z339)
† Corresponding author. Email: wangliang06@semi.ac.cn
Received 23 February 2008, revised manuscript received 7 April 2008

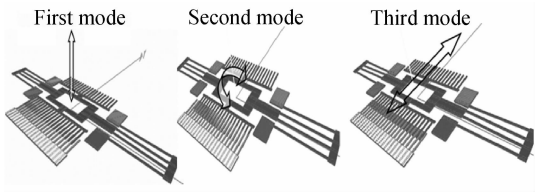

Fig. 2 Vibrating modes of the folded-beam resonators Arrows indicate direction of vibration.

For force components along the x-direction, as shown in Fig. 1, we have:

$$F_x = -\frac{V^2}{2} \times \frac{\partial}{\partial x}\left(\frac{\varepsilon_0 xt}{d}\right) = -\frac{\varepsilon_0 t}{2d}V^2 \qquad (2)$$

where ε_o is the dielectric constant, d is the gap between the plates, and t is the thickness of the plate. In Eq. (2), $-\frac{\varepsilon_0 t}{2d}$ is a constant, which is independent of the lateral displacement (x) when x is less than the finger overlap (Fig. 1). Therefore, electrostatic-comb drives can have linear electromechanical transfer functions for large displacements, in contrast to parallel-plate capacitive drives.

2.2 Resonant structure design

Motions for these trusses suspension are capable of relief of the built-in residual strain in the structural film. Both the average residual stress in the poly 3C-SiC film and the stress induced by large-amplitude plate motion should be largely relieved by this design[6]. In addition, the long effective support lengths result in a highly compliant suspension. Plates with a 100μm-long folded-beam resonate with amplitudes as large as 5μm.

Figure 2 illustrates the first three vibrating modes of the folded-beam resonator. In the first mode, the vibrating direction is vertical to the plate plane. The second mode is a torsional resonant form. The third mode is in-plane vibration. Because of electrostatic restriction, the resonator only works in the third mode.

In the third in-plane vibrating mode, the trusses of the folded-beam displace at half the velocity of the plate (seen in Fig. 3) and the displacements distributing along the beam length direction are given by Ref. [7].

$$x_1(y) = \frac{x_0}{2}\left[3\left(\frac{y}{L}\right)^2 - 2\left(\frac{y}{L}\right)^3\right]$$
$$x_2(y) = x_0 - x_t(y) \qquad (3)$$

where x_0 is the maximum displacement of the plate and L is the beam length.

The resonant frequency of the sensor is analytically calculated using Rayleigh's method based on the third mode[8]:

$$\mathrm{KE}_{max} = \mathrm{PE}_{max} \qquad (4)$$

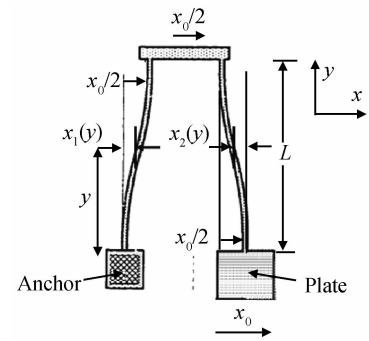

Fig. 3 Third mode shape of a folded-beam when the resonant plate is displaced by x_0

where KE_{max} is the maximum kinetic energy during a vibration cycle and PE_{max} is the maximum potential energy.

$$\mathrm{KE}_{max} = \mathrm{KE}_{plate} + \mathrm{KE}_{truss} + \mathrm{KE}_{beam}$$
$$= -\frac{1}{2}v_p^2 M_p + \frac{1}{2}v_t^2 M_t + \frac{1}{2}\int v_b^2 \mathrm{d}M_b \qquad (5)$$

where M_p is the plate mass, M_t is the mass of the folding trusses, and M_b is the total mass of the suspension beams.

$$\mathrm{KE}_{max} = \frac{1}{2}x_0^2\omega^2 M_p + \frac{1}{8}x_0^2\omega^2 M_t + \frac{\omega^2}{2}\int x(y)\mathrm{d}M_b$$
$$= x_0^2\omega^2\left(\frac{1}{2}M_p + \frac{1}{8}M_t + \frac{6}{35}M_b\right) \qquad (6)$$

$$\mathrm{PE}_{max} = \int_0^{x_0} F_x dx = \int_0^{x_0} k_x x \mathrm{d}x = \frac{1}{2}k_x x_0^2 \qquad (7)$$

And k_x is given by Ref. [6].

$$k_x = Eh\left(\frac{W}{L}\right)^3 \qquad (8)$$

where W and h are the cross-sectional width and thickness, respectively. Then the expression for the resonance frequency (f_r) becomes:

$$f_r = \frac{1}{2\pi}\left[\frac{2Eh(W/L)^3}{\left(M_P + \frac{1}{4}M_t + \frac{12}{35}M_b\right)}\right]^{1/2} \qquad (9)$$

From Eq. (9), the f_r can be improved through adjusting the beam width, beam length, plate area, and selecting a high Young's modulus material to process.

2.3 Finite-element analysis

Finite-element analysis is performed using Intellisuite software, available commercially from IntelliSense Incorporated. The Intellifab module of the Intellisuite software is introduced to build the resonant structure through simulating the processes of the resonator device. The device performance is analyzed using the ThermoElectroMechanical module. Details of the overall design are summarized in Table 1.

The Young's modulus of poly 3C-SiC can be obtained from Eq. (9), the geometry, and the measured resonant frequency.

Table 1　Parameters of the resonator

Parameter	Value	Unit
Folded-beam length, L	100	μm
Folded-beam width, W	2/3.5/5.5	μm
Structural layer thickness, h	3	μm
No. finger overlaps	20	—
Finger gap space, d	2	μm
Finger overlap length, L_d	20	μm
Young's modulus, E	430(calculated)	GPa
Density of poly 3C-SiC, ρ	3.2	g/cm^3

Figure 4 shows the dependence of simulated resonant frequencies versus the Young's modulus and the beam length. The simulated resonant frequency increases rapidly as the Young's modulus is enhanced (as seen in Fig. 4(a)). Poly 3C-SiC with high Young's modulus are more profitable to fabricate the high frequency resonator. An inverse relationship between frequency and beam length was obtained, as seen in Fig. 4(b).

The simulated frequency does not change with the beam thickness. However, when the W/h ratio exceeds 2, the resonator can not vibrate in the lateral direction. Thus, adjusting the resonant frequency by increasing the beam width is also affected by the beam thickness.

3　Fabrication and measurement

The resonators with three different beam widths

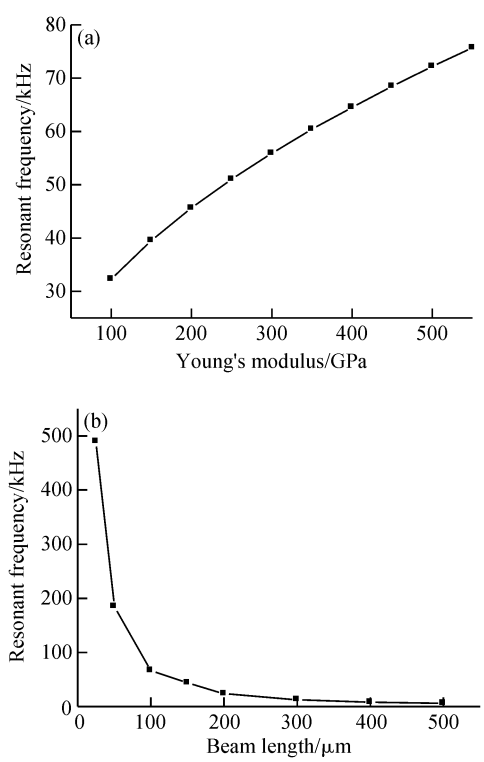

Fig. 4　Dependence of simulated resonant frequency versus the Young's modulus (a) and the beam length (b)

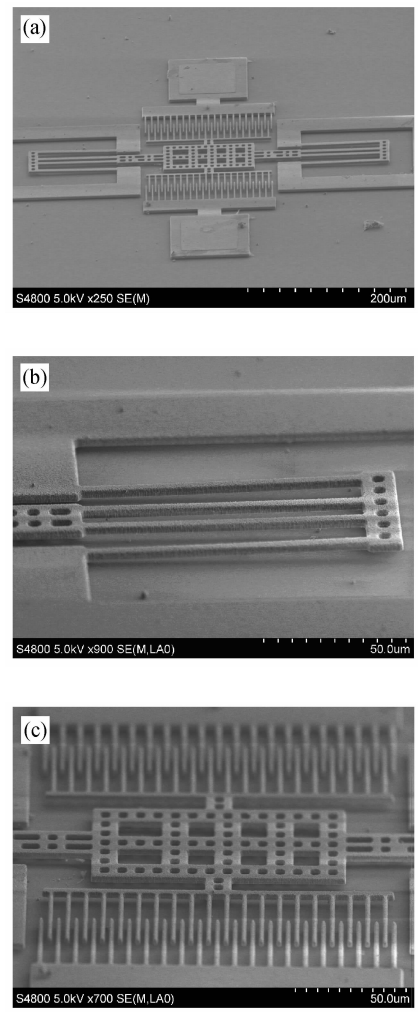

Fig. 5　SEM of the fabricated poly 3C-SiC resonator structure (a) Full view; (b) Enlarged view of the folded-beam structure; (c) Enlarged view of the linear comb structure and the plate

were fabricated using 3μm thick poly 3C-SiC thin film grown on PECVD SiO_2/ Si_3N_4/SiO_2/Si substrates in a hot-wall, RF-induction heated LPCVD reactor. The experimental setup was described in Ref. [9]. SiO_2 was used as isolation and sacrificial layers separately in the device structure. A Si_3N_4 layer was grown between the two SiO_2 layers to enhance the isolation effect and to protect the SiO_2 layer under it. The thermal evaporated Ni film was deposited on poly 3C-SiC to form an Ohmic contact by annealing at 1000℃ in a vacuum environment. Cr/Au were deposited as pad metals[9].

The resonator structure is shown in Fig. 5. The beam widths are 2, 3.5, and 5.5μm, respectively. The other parameters are the same as in Table 1. Dynamic behaviors of the devices were measured by a MEMS micro-motion analyzer system.

Figure 6 shows the dependence of the simulated and measured resonant frequencies on the beam width. The resonant frequency increases as the beam width increases. The measured resonant frequencies of

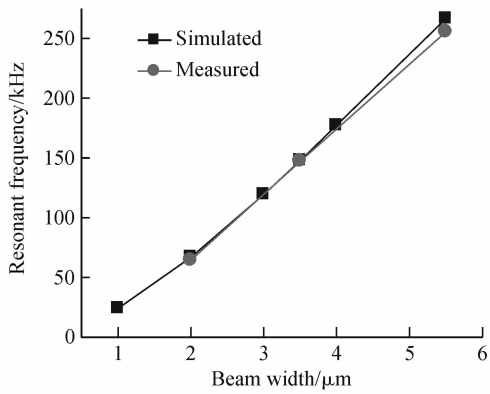

Fig. 6 Dependence of the simulated and measured resonant frequencies on the beam width

the 2, 3.5, and 5.5μm in beam width resonators are 64.5, 147.4, and 255.5kHz, respectively, which are in good agreement with the simulated resonant frequencies.

4 Conclusion

A numerical solution based on the Rayleigh's method was used to determine the resonance frequencies. The resonance frequencies for the resonators are governed mainly by their material properties such as the Young's modulus and resonator geometry parameters such as beam width, length, thickness, and the area of the plate. Resonators with three difference beam widths were fabricated. Their resonant frequencies were measured to be 64.5, 147.2, and 255.5kHz, respectively, which is in good agreement with the simulated resonant frequencies. It was shown that an improved frequency performance could be obtained on the poly 3C-SiC thin films with high Young's modulus.

Acknowledgements The authors would like to thank assistant professor Hu Xiaodong and his colleagues from the State Key Laboratory of Precision Measuring Technology and Instruments in Tianjin University for their contributions to the measurement of the resonator.

References

[1] Nguyen T C H. High-Q micromechanical oscillators and filters for communications. IEEE Int Symp Circuits and Systems, 1997: 2825
[2] Fleischman A J, Roy S, Zorman C A, et al. Behavior of polycrystalline SiC and Si surface-micromachined lateral resonant structure at elevated temperature. Proc Int Conf Silicon Carbide, Ⅲ-Nitrides and Related Materials, 1997: 889
[3] Tang W C, Nguyen T C H, Judy M W, et al. Electrostatic-comb drive of lateral polysilicon Resonators. Sensors and Actuators, 1990, 21～23: 328
[4] Roy S, DeAnna R G, Zorman C A, et al. Fabrication and characterization of polycrystalline SiC resonators. IEEE Trans Electron Devices, 2002, 49: 2323
[5] Yang Y T, Ekinci K L, Huang X M H, et al. Monocrystalline silicon carbide nanoelectromechanical systems. Appl Phys Lett, 2001, 78: 162
[6] Tang W C, Nguyen T C H, Howe R T. Laterally driven polysilicon resonant microstructures. Sensors and Actuators, 1989, 20: 25
[7] Gere J M, Timoshenko S P. Mechanics of materials. 2nd ed. Belmont: Wadsworth, 1984
[8] Hove R T. Resonant microsensors. Technical Digest, 4th International Conference on Solid-State Sensors and Actuators, Tokyo, Japan, 1987: 843
[9] Ning J, Sun G, Gong Q, et al. Fabrication of poly crystalline 3C-SiC resonator. 8th International Conference on Solid-State and Integrated Circuit Technology Proceedings, Shanghai, 2006: 572

水平静电驱动式多晶 3C-SiC 折叠悬臂梁谐振器微结构*

王 亮[1,2,†] 赵永梅[1,2] 宁 瑾[2] 孙国胜[1,2] 王 雷[1] 刘兴坊[1,2] 赵万顺[1] 曾一平[1] 李晋闽[1]

(1 中国科学院半导体研究所 新材料中心，北京 100083)
(2 中国科学院传感技术国家重点实验室，北京 100083)

摘要： 介绍了一种微机械叉指静电驱动折叠悬臂梁谐振器的设计和制作方法. 将 Rayleigh 分析法和有限元分析法结合起来分析调整器件尺寸和材料参数对器件性能的影响. 制作了三种不同悬臂梁宽度的微机械横向谐振器件，经实验检测它们的谐振频率分别为 64.5, 147.2, 255.5kHz, 与模拟结果符合得很好. 该结果显示由于具有很高的杨式模量，利用多晶 3C-SiC 材料体系制作的谐振器件能够具有更高的谐振频率.

关键词： 横向谐振器件；折叠悬臂梁；叉指结构；微机械系统；谐振器；碳化硅
EEACC： 2575
中图分类号： TN303 **文献标识码：** A **文章编号：** 0253-4177(2008)08-1453-04

* 国家自然科学基金(批准号：60406010) 和国家高技术研究发展计划(批准号：2006AA04Z339)资助项目
† 通信作者. Email: wangliang06@semi.ac.cn
2008-02-23 收到，2008-04-07 定稿